5

Nanotechnology With S-Layer Proteins

Bernhard Schuster, Erica Györvary, Dietmar Pum, and Uwe B. Sleytr

Summary

The cross-fertilization of biology, chemistry, material sciences, and solid-state physics is opening up a great variety of new opportunities for innovation in nanosciences. One of the key challenges is the technological utilization of self-assembly systems wherein molecules spontaneously associate under equilibrium conditions into reproducible supramolecular aggregates. The attractiveness of such processes lies in their capability to build uniform, ultrasmall functional units and the possibility of exploiting such structures at meso- and macroscopic scale for life and nonlife science applications. The use of crystalline bacterial cell-surface proteins (S-layer proteins) provided innovative approaches for the assembly of supramolecular structures and devices with dimensions of a few to tens of nanometers. S-layers have proven to be particularly suited as building blocks in a molecular construction kit involving all major classes of biological molecules. The immobilization of biomolecules in an ordered fashion on solid substrates and their controlled confinement in definite areas of nanometer dimensions are key requirements for many applications including the development of bioanalytical sensors, biochips, molecular electronics, biocompatible surfaces, and signal processing among functional membranes, cells, and integrated circuits.

Key Words: Surface layers; S-layers; two-dimensional protein crystals; biomimetics; self-assembly; nanotechnology; nanobiotechnology; nanoparticle; construction kit; supported lipid membranes.

1. Introduction

Many prokaryotic organisms have regular arrays of (glyco)proteins on their outermost surface (for a compilation, *see* **ref. *1***). These monomolecular crystalline surface layers, termed S-layers ***(2)***, are found in members of nearly every taxonomic group of walled bacteria and cyanobacteria and represent an almost universal feature of archaeal cell envelopes (*see* **Fig. 1**). S-layers are generally composed of a single protein or glycoprotein species with a molecular mass of

From: *Methods in Molecular Biology, vol. 300:*
Protein Nanotechnology, Protocols, Instrumentation, and Applications
Edited by: T. Vo-Dinh © Humana Press Inc., Totowa, NJ

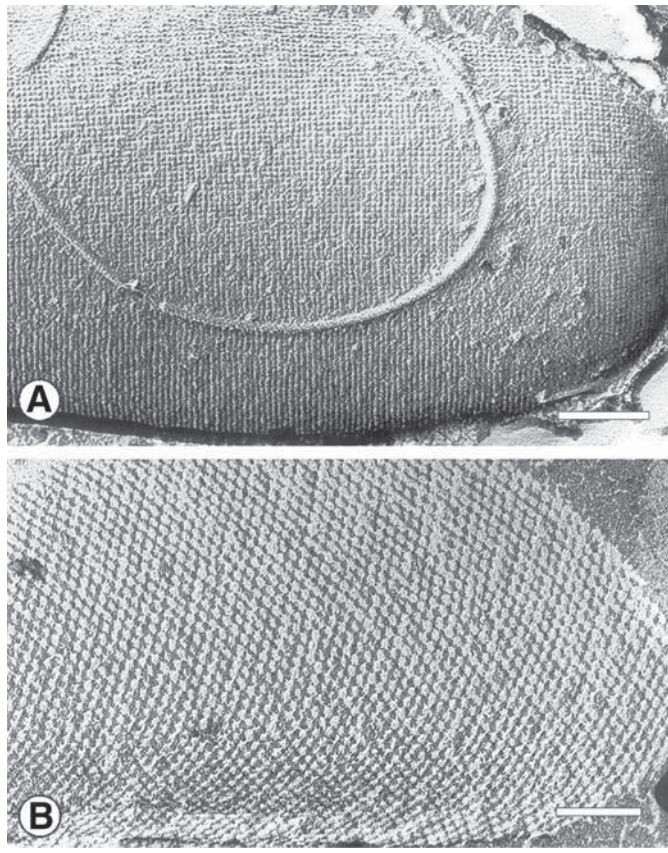

Fig. 1. Electron micrographs of freeze-etching preparations of whole cells of **(A)** *B. sphaericus*, showing a square S-layer lattice; **(B)** *Thermoplasma thermohydrosulfuricus*, revealing a hexagonally ordered array. Bars: **(A)** 200 nm; **(B)** 100 nm. (Reprinted from **ref. *45*** with permission from the publisher; © 2001, Elsevier Science.)

40,000 to 230,000 Daltons and exhibit either oblique (p1, p2), square (p4), or hexagonal (p3, p6) lattice symmetry with unit cell dimensions in the range of 3 to 30 nm (*see* **Fig. 2**). One morphological unit consists of one, two, three, four, or six identical subunits, respectively. The monomolecular arrays are generally 5 to 10 nm thick and show pores of identical size (diameter of 1.5–8 nm) and morphology. In most S-layers, the outer face is less corrugated than the inner face. Moreover, S-layers are highly anisotropic structures regarding the net charge and hydrophobicity of the inner and outer surface ***(3,4)***. Owing to the crystalline character of S-layers, functional groups (e.g., carboxyl, amino, hydroxyl groups) are repeated with the periodicity of the protein lattice.

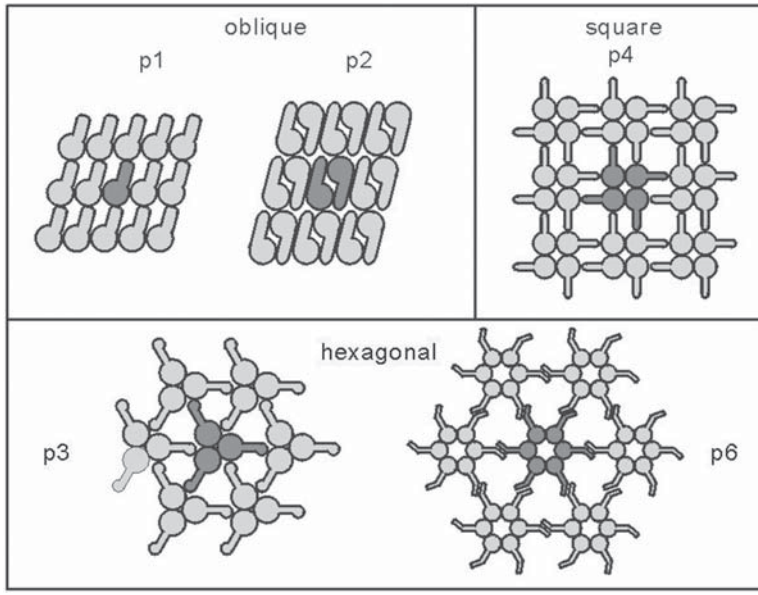

Fig. 2. Schematic representation of types of S-layer lattice grouped according to possible 2D space group symmetries. Morphological units were chosen arbitrarily and are shown in dark gray. (Reprinted from **ref. *8*** with permission from the publisher; © 2003, Wiley-VCH.)

Because S-layers possess a high degree of structural regularity and the constituent subunits are the most abundant of all bacterial cellular proteins, these crystalline arrays are excellent models for studying the dynamic aspects of assembly of a supramolecular structure in vivo and in vitro. Moreover, the use of S-layers provided innovative approaches for the assembly of supramolecular structures and devices. S-layers have proven to be particularly suited as building blocks and patterning elements in a biomolecular construction kit involving all major classes of biological and chemically synthesized molecules or nanoparticles. In this context, one of the most important properties of isolated S-layer (glyco)protein subunits is their capability to reassemble into monomolecular arrays in suspension, at the air interface, on a solid surface, on floating lipid monolayers (*see* **Fig. 3**), and on liposomes or particles (for a review, *see* **refs. *5–8***).

An important line of development in S-layer-based technologies is presently directed toward the genetic manipulation of S-layer proteins. These strategies open new possibilities for the specific tuning of their structure and function. S-layer proteins incorporating specific functional domains of other proteins while maintaining the self-assembly capability will lead to new ultrafiltration

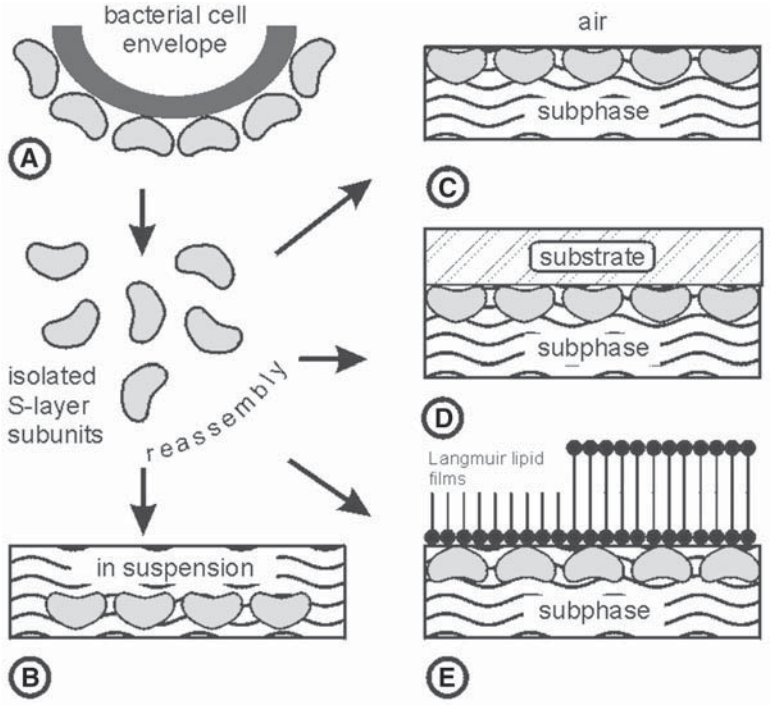

Fig. 3. **(A)** Schematic illustration of recrystallization of isolated S-layer subunits into crystalline arrays. The self-assembly process can occur **(B)** in suspension, **(C)** at the air-liquid interface, **(D)** on solid supports, and **(E)** on Langmuir lipid films. (Reprinted from **ref. *5*** with permission from the publisher; © 1999, Wiley-VCH.)

membranes, affinity structures, enzyme membranes, metal-precipitating matrices, microcarriers, biosensors, diagnostics, biocompatible surfaces, and vaccines ***(6,7)***.

Although up to now most S-layer technologies developed concerned life sciences, an important emerging field of future applications relates to nonlife sciences. Native or genetically modified S-layers recrystallized on solid supports can be used as patterning elements for accurate spatial positions of nanometer-scale metal particles or as matrices for chemical deposition of metals as required for molecular electronics and nonlinear optics.

2. Materials

2.1. Bacterial Strain, Growth in Continuous Culture, and Isolation

2.1.1. Bacterial Strains

1. *Geobacillus stearothermophilus* PV72, kindly provided by F. Hollaus (Österreichisches Zuckerforschungsinstitut, Tulln, Austria).

2. *Bacillus sphaericus* CCM 2177 (Czech Collection of Microorganisms, Brno, Czech Republic).

2.1.2. Growth in Continuous Culture

1. SVIII medium: 10 g/L of peptone, 5 g/L of yeast extract, 5 g/L of lab lemco, 1.2 g/L of $K_2HPO_4 \cdot 3H_2O$, 0.1 g/L of $MgSO_4 \cdot 7H_2O$, 0.6 g/L of sucrose.
2. Bioreactor type Biostat E (Braun, Melsungen, Germany).
3. Mass flow controller (Brooks, Veenendaal, The Netherlands).
4. 1 *N* NaOH and 2 *N* H_2SO_4 (Merck, Darmstadt, Germany).
5. pH and redox probes of gel paste type and an amperometric probe (Ingold, Urdorf, Switzerland).
6. Spectrophotometer (model 25; Beckman, Fullerton, CA).
7. Sodium dodecyl sulfate-polyacrylamide gel electrophoresis (SDS-PAGE) apparatus (Bio-Rad, Hercules, CA).
8. Densitometer (Elscript 400AT/SM; Hirschmann, Neuried, Germany).
9. Centrifuge (Sepatech 17RS; Heraeus, Hanau, Germany).
10. Buffer A: 50 m*M* Tris-HCl (Fluka, Buchs, Switzerland) buffer, adjusted to pH 7.2.

2.1.3. Preparation of Cell-Wall Fragments

1. Ultrasonicator treatment (Ultrasonics Sonicator W-385; Farmingdale, NY).
2. Centrifuge (JA-HS; Beckmann).
3. 0.75% Triton X-100 (Serva, Heidelberg, Germany) dissolved in buffer A.

2.1.4. Isolation of S-Layer Proteins

1. 5 *M* Guanidine hydrochloride (Fluka) in buffer A.
2. Ultracentrifuge (Beckmann L5-65).
3. 10 m*M* $CaCl_2$ in distilled water (Fluka).
4. Dialysis tube with a cutoff of 12 to 16 kDa and a pore size of 25 Å (Biomol, Hamburg, Germany).
5. Spectrophotometer (Hitachi U 2000; Tokyo, Japan).

2.2. S-Layer Proteins on Solid Supports

2.2.1. Solid Supports

1. Silicon nitride and silicon wafers (100 orientation, p-type, boron-doped, resistivity of 25 to 45 Ωcm, native oxide layer; MEMC, Novara, Italy, or Wacker Chemitronic, Burghausen, Germany).
2. Metallic wafers: gold-coated supports (Pharmacia, Peapack, NJ), titanium, aluminum, palladium.
3. Polymers: polyester, polypropylene, poly(ethylene terephthalate), poly(methacrylic acid methylester), polycarbonate (Wettlinger Kunststoffe, Wien, Austria).

4. Glass slides (Assistant Micro Slides, No. 2400; Elka, Sondheim, Germany), cellulose, mica, highly oriented pyrolytic graphite.

2.2.2. Cleaning and Modification of Solid Supports

1. Solvents (acetone, propan-2-ol, ethanol, ammonia [29%], hydrogen peroxide [30%], HCl [37%], and dried toluene; Merck), Milli-Q water (Millipore, Bedford, MA), and N_2 gas (Linde, Wien, Austria).
2. Silanes: octadecyltrichlorosilane, (3-methacryloyloxypropyl)-trimethoxysilane, trimethoxysilane, decyldimethylsilane, hexamethyldisilane, 2-aminopropyltrimethoxysilane, 3-mercaptopropyltrimethoxysilane (ABCR, Karlsruhe, Germany).
3. Plasma cleaner (Gala, Bad Schwalbach, Germany) and O_2 gas (Linde).
4. Kruess contact angle measurement system G1 (Hamburg, Germany).

2.2.3. Crystallization of S-Layer Proteins on Solid Supports

1. Buffer B: 1 m*M* citrate buffer (Fluka) adjusted to pH 4.0 with NaOH and HCl (Merck).
2. Buffer C: 10 m*M* $CaCl_2$ in 0.5 m*M* Tris-HCl (Fluka) buffer adjusted to pH 9.0 with NaOH and HCl (Merck).
3. pH Meter (Mettler Toledo MP 220; Schwerzenbach, Switzerland).
4. *G. stearothermophilus* PV72 (0.1 mg/mL) (*see* **Subheading 2.1.1.**) in buffer B.
5. *B. sphaericus* CCM 2177 (0.1 mg/mL) (*see* **Subheading 2.1.1.**) in buffer C.
6. Rotator (Reax2; Heidolph, Schwabach, Germany).

2.2.4. Atomic Force Microscopy

1. Digital Instruments Nanoscope IIIa (Santa Barbara, CA) or other nanoscope with an E-scanner (nominal scan size: 12 µm) or a J-scanner (nominal scan size: 130 µm).
2. Standard 200-µm-long oxide-sharpened silicon nitride cantilevers (NanoProbes; Digital Instruments) with a nominal spring constant of 0.06 Nm^{-1}.

2.3. Patterning of Crystalline S-Layer Proteins

2.3.1. S-Layer Protein-Covered Solid Supports

1. S-layer protein SbpA of *B. sphaericus* CCM2177 (*see* **Subheading 2.1.1.**).
2. Buffer C (*see* **Subheading 2.2.3.**).
3. Cleaning and characterization materials (*see* **Subheading 2.2.2.**).

2.3.2. Lithographic Masks

1. Chromium coating 100 nm thick on quartz glass consisting of lines and squares (feature sizes ranging from 200 to 1000 nm) with different line-and-space ratios.

2.3.3. Excimer Laser

1. ArF excimer laser (model EMG 102E; Lambda Physik, Göttingen, Germany).

2.3.4. Poly(dimethylsiloxane) Molds

1. Silicon mold master: 4-in. silicon wafers, photoresist (Clariant AZ 9260; Microchemicals, Ulm, Germany), photolithography.
2. Poly(dimethylsiloxane) (PDMS) (Sylgard 184; Dow Corning, Midland, MI).
3. Oven (Memmert, U 25; Schwabach, Germany), exsiccator.

2.3.5. Microscopy

1. Materials for atomic force microscopy (AFM) (*see* **Subheading 2.2.4.**).
2. Materials for epifluorescence microscopy:
   a. Buffer D: 0.1 *M* $NaHCO_3$-Na_2CO_3 buffer adjusted to pH 9.2 with NaOH and HCl (Merck).
   b. Fluorescence marker (fluorescein isothiocyanate [FITC]), and dimethyl sulfoxide (DMSO) (both from Sigma-Aldrich, Wien, Austria).
   c. Fluorescence microscope (Nikon, Tokyo, Japan).

2.4. Formation of Nanoparticle Arrays

2.4.1. Preparation of Supports

1. Standard formvar- and carbon-coated electron microscope grids (Groepl, Tulln, Austria).
2. SiO_2, to coat grids by evaporation (EPA 100; Leybold-Heraeus, Köln, Germany).
3. O_2 plasma, to treat SiO_2-coated grids in a plasma cleaner (*see* **Subheading 2.2.2.**).

2.4.2. Electrostatic Binding of Nanoparticles to S-Layers

1. S-layer protein SbpA of *B. sphaericus* CCM 2177 (0.1 mg/mL) in buffer C (*see* **Subheading 2.2.3.**) and O_2-treated SiO_2-coated grids.
2. Nanoparticles: citrate-stabilized gold nanoparticles (mean diameter of 5 nm; Sigma-Aldrich) and amino-modified cadmium selenide (CdSe) nanoparticles (mean diameter of 4 nm; University of Hamburg, Germany).

2.4.3. Transmission Electron Microscopy

1. Uranyl acetate (2.5% in Milli-Q water; Merck) for negative staining.
2. Transmission electron microscope (TEM CM12; Philips, Eindhoven, The Netherlands).

2.5. S-Layer-Supported Lipid Membranes

2.5.1. Painted and Folded Membranes

1. 1,2-Diphytanoyl-*sn*-glycero-3-phosphocholine (DPhyPC) (Avanti, Alabaster, AL).
2. Hexadecane, *n*-decane, *n*-hexane, and pentane (Fluka).
3. Chloroform and ethanol (Merck).
4. Electrolyte: 0.01 to 1 *M* KCl or NaCl in Milli-Q water and, if desired, 10 m*M* $CaCl_2$ (all chemicals obtained from Merck).

5. Painted membranes: homemade Teflon chamber with a drilled orifice, 0.9 mm in diameter, dividing the two compartments with a volume of about 12 mL each (for more details, *see* **refs. *9–11***).
6. Copper wire (approx 1 mm in diameter) covered with a Teflon (polytetrafluoroethylene) tube and bent in an L shape to form a brush.
7. Folded membranes: homemade Teflon chamber with a Teflon film (25 µm thick; Goodfellow, Cambridge, England) which divided the two compartments with a volume of about 3.5 mL, each. Into the Teflon film a hole, approx 140 µm in diameter, was punched by a perforating tool (syringe needle that has been sharpened inside and outside; for further details *see* **refs. *9***, ***10***, ***12***).
8. Two 1-mL single-use syringes (B. Braun, Melsungen, Germany), or others, two plastic tubes.

2.5.2. Technical Equipment

1. Patch-clamp amplifier (EPC9; HEKA, Lamprecht, Germany), or others, with corresponding software (Pulse+PulseFit 8.11; HEKA).
2. Two silver/silver chloride (Ag/AgCl) electrodes (*see* **Note 1**).
3. Vibration isolation unit (Newport, Darmstadt, Germany) with a Faraday cage on top.

3. Methods

3.1. Bacterial Strain, Growth in Continuous Culture, and Isolation

3.1.1. Growth in Continuous Culture

G. stearothermophilus PV72 ***(3,13,14)*** was grown on 50 mL of SVIII medium ***(15)*** in a 300-mL shaking flask at 57°C to mid-logarithmic growth. Two hundred milliliters of this suspension was used as the inoculum for 5 L of SVIII medium sterilized in a bioreactor. Before inoculation, 20 mL of a sterile glucose solution (6 g of glucose in total) was added. Cultivation was performed at 57°C and a stirring speed of 300 rpm. In continuous culture, the dilution rate was kept at 0.1 h^{-1}. The rate of aeration was 0.5 L of air/min. The pH of the culture was kept at 7.2 ± 0.2 by the addition of either 1 *N* NaOH or 2 *N* H_2SO_4. Aeration rate was controlled by a mass flow controller. Redox potential was measured by a platinum contact redox probe. The partial oxygen pressure was monitored with an amperometric probe. The cell density was measured at 600 nm in a spectrophotometer. In principle, *B. sphaericus* CCM 2177 ***(16)*** was cultivated under the same conditions, but because this organism is a mesophilic one, the temperature was lowered to 32°C (*see* **Note 2**).

For controlling the homogeneity of the culture, 10-mL samples were taken from the bioreactor at different times. Aliquots were plated on SVIII agar, and the grown biomass (at 57°C for 18 h) was used for SDS-PAGE ***(13)***. The gel system contained a 4% stacking gel and a 10% separation gel. Single-cell colonies grown on SVIII agar plates were subjected to SDS-PAGE for final identi-

fication. The relative amounts from both types of S-layer proteins were estimated from SDS gels by densitometric evaluation.

For biomass harvesting, the culture suspension from the overflow of continuous culture was collected in heat-sterilized bottles at 2 to 4°C. Cells were separated from spent medium by continuous centrifugation at 16,000*g* and 4°C, washed with buffer A, and stored at –20°C.

3.1.2. Preparation of Cell-Wall Fragments

The frozen biomass (100 g) was suspended in 350 mL of buffer A. The suspension was separated into three parts and the cells were broken by ultrasonic treatment for 2 min at maximal output. To avoid autocatalytic processes, all preparation steps must be done on ice at 4°C. Subsequently, the intact and broken cells were separated by centrifuging at 28,000*g* for 10 min. The upper, lighter pellet was detached and collected. The lower, darker pellet was again suspended in buffer A, ultrasonically treated, and sedimented. This procedure was repeated four times. To remove contaminating plasma membrane fragments, the crude cell-wall preparations (collected pellets) were extracted with 250 mL of 0.75% Triton X-100 (dissolved buffer A) and stirred for 10 min at room temperature (22 ± 2°C). Subsequently, the cell-wall fragments were sedimented at 40,000*g* for 10 min. The extraction step was repeated three times. Finally, the pellet was frozen in aliquots at –20°C.

3.1.3. Isolation of S-Layer Proteins

Cell-wall fragments (2 mg) were suspended in 30 mL of guanidine hydrochloride solution in buffer A and stirred at room temperature for 30 min. Subsequently, the suspension was sedimented at 30,000 rpm and 4°C for 45 min in an ultracentrifuge. The supernatant was dialyzed either against a $CaCl_2$ solution (*G. stearothermophilus* PV72) or against distilled water (*B. sphaericus* CCM 2177) three times for at least 2 h each, at 4°C (*see* **Note 3**). Finally, the S-layer self-assembly products (*see* **Note 4**) were sedimented for 15 min at 40,000*g* and 4°C. The supernatant containing single subunits and oligomeric precursors were stored at 4°C and used within 5 d. For determination of the protein concentration, the measured adsorption at 280 nm was multiplied by 1.75 and 1.64 for the S-layer protein SbsB of *G. stearothermophilus* PV72 and SbpA of *B. sphaericus* CCM 2177, respectively. The protein solutions were adjusted to a concentration of 1 mg of protein/mL and used for all recrystallization experiments described later (**Fig. 3**).

3.2. S-Layer Proteins on Solid Supports

3.2.1. Preparation of Solid Supports

Silicon wafers were immersed in hot acetone followed by rinsing in propan-2-ol and finally washed with ethanol and Milli-Q water. The advancing contact

angle of water on the clean silicon surface was 65°. To increase the hydrophilicity of the substrates, the silicon wafers were treated in an O_2 plasma (20-s leaning time, 0.01-bar plasma pressure, 70% power density, high-purity-grade O_2). The plasma-treated silicon substrates with an advancing contact angle of water of 5° were used immediately for the recrystallization studies. Other solid supports (e.g., metals, polymers, glass) were only rinsed with ethanol and Milli-Q water before use.

Silanization procedures (solution or vapor phase) using different silanes were applied to obtain silicon or glass substrates with more-hydrophobic surfaces ***(17,18)***. The substrates were cleaned in a solution containing 1:1:5 parts of ammonia (29%), hydrogen peroxide (30%), and Milli-Q water at 80°C for 10 min. Subsequently, the silicon or glass substrates were treated with 1:1:6 parts of concentrated hydrogen chloride (37%), hydrogen peroxide (30%), and deionized water at 80°C for 15 min. Finally, the substrates were rinsed thoroughly with Milli-Q water and dried in a stream of nitrogen gas. This procedure is known as RCA cleaning.

For silanization out of a solution, the substrates were further rinsed with acetone and dried with toluene. Subsequently, the supports were put into anhydrous toluene containing 1% silane. Silanization (e.g., with decyldimethylsilane), was carried out for 30 min to 2 h with mild shaking at room temperature. Finally, the silanized supports were rinsed with toluene, methanol, and Milli-Q water.

Silanization from vapor phase was performed with silanes of shorter chain lengths (e.g., hexamethyldisilane). Supports were baked with some drops of silane in an airtight glass vessel at 60°C for 2 h and finally rinsed with methanol.

3.2.2. S-Layer Protein Recrystallization on Solid Supports

For recrystallization of the S-layer protein SbsB of *G. stearothermophilus* PV72 and SbpA of *B. sphaericus* CCM 2177, buffer B and buffer C were used, respectively. The protein concentration in all experiments was 0.1 mg/mL. Recrystallization on solid supports was carried out either in rotating Eppendorf tubes that had been previously filled with the protein solution or in glass wells. In the latter case, the substrates were placed onto the air-liquid interface. After a recrystallization time of 4 h at room temperature, the supports were removed by tweezers, washed, and stored in Milli-Q water (4°C).

3.2.3. Atomic Force Microscopy

Scanning was carried out in contact mode in a liquid cell filled with a 100 m*M* NaCl solution (**Fig. 4**). The applied force was kept to a minimum during scanning to prevent modification of the sample surface by the tip. Scan speed was approx 6 Hz. Images were flattened line by line during recording using the microscope's software.

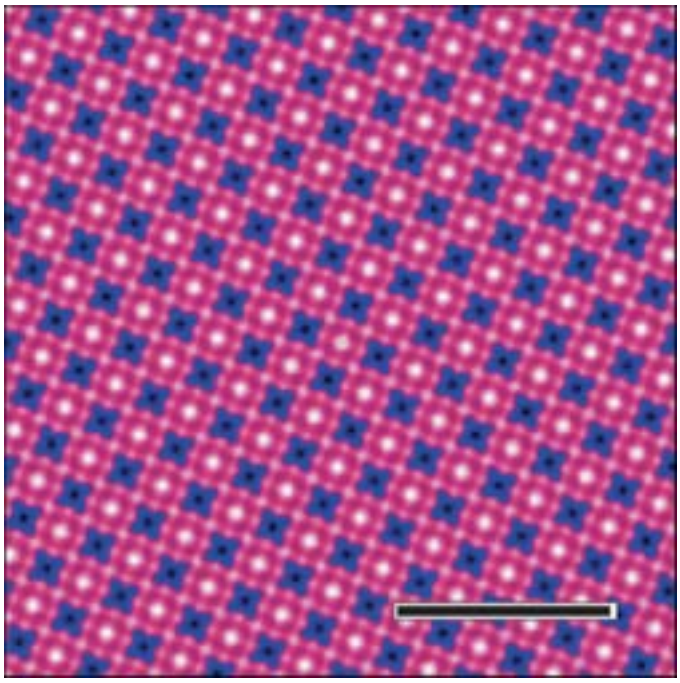

Fig. 4. Scanning force microscopic image of S-layer protein SbpA from *B. sphaericus* CCM 2177 recrystallized on a silicon wafer. The image was recorded in contact mode in a liquid cell (bar = 50 nm). (Reprinted from **ref. *8*** with permission from the publisher; © 2003, Wiley-VCH.)

AFM studies showed crystalline domains with average diameters of 10 to 20 µm for SbsB and 0.1 to 10 µm for SbpA, when crystallized on a variety of solid supports (*see* **Table 1**). In particular, SbsB generated crystalline monolayers only on hydrophobic solid supports, whereas SbpA formed extended crystalline domains on hydrophilic surfaces, but only small patches on hydrophobic ones.

3.3. Patterning of Crystalline S-Layer Proteins

3.3.1. Excimer Laser Patterning

Silicon wafers were cleaned with several solvents and O_2 plasma treated (*see* **Subheading 3.2.**). Recrystallization of isolated S-layer protein on the silicon wafer was carried out as previously described (*see* **Subheading 3.2.**).

Prior to irradiation, the recrystallized S-layer was carefully dried in a stream of high-purity nitrogen gas in order to remove excess water not required for maintaining the structural integrity of the protein lattice (*see* **Note 5**). Then, the

Table 1
Supports and Their Modifications
Used in Formation of Crystalline S-Layer Protein Layers[a]

Support	Surface and modifications	SbsB	SbpA
Silicon wafers (100 orientation, p-type)	Si (native oxide layer) RCA cleaned	–	–
	Si (native oxide layer)	+	+[b]
	Si (native oxide layer) O_2 plasma treated	–	+
	Si3N4	+	+
	Octadecyltrichlorosilane	+	+
	(3-Methacryloyloxypropyl)-trimethoxysilane	+	+
	Trimethoxysilane	+	+
	Decyldimethylsilane	+	+
	Hexamethyldisilane	+	+
	2-Aminopropyltrimethoxysilane	+	+
	3-Mercaptopropyltrimethoxysilane	+	+
Metallic supports	Gold	+	+
	Titanium	+	+
	Aluminum	n	+
	Palladium	+	+
Polymers	Polyester	+	n
	Polypropylene	+	+
	Poly(ethylene terephthalate)	n	+
	Poly(methacrylic acid methylester)	n	+
	Polycarbonate	+	n
Others	Glass	+	+
	Cellulose	+	+
	Mica	–	+
	Highly oriented pyrolytic graphite	–	+

[a]+, crystallization; –, no crystallization; n, not tested.
[b]Very large crystalline domains.

lithographic mask was brought into direct contact with the S-layer-coated silicon wafer (**Fig. 5**). The whole assembly was irradiated by the ArF excimer laser (*see* **Note 6**) in a series of one to five pulses with an intensity of about 100 mJ/cm^2 per pulse (pulse duration: 8 ns; 1 pulse/s). Finally, the mask was removed and the S-layer-coated silicon wafer was immediately immersed in buffer.

S-layers that have been patterned by ArF excimer laser radiation may also be used as high-resolution etching masks in nano/microlithography. This application requires enhancement of the patterned protein layer by electro-less

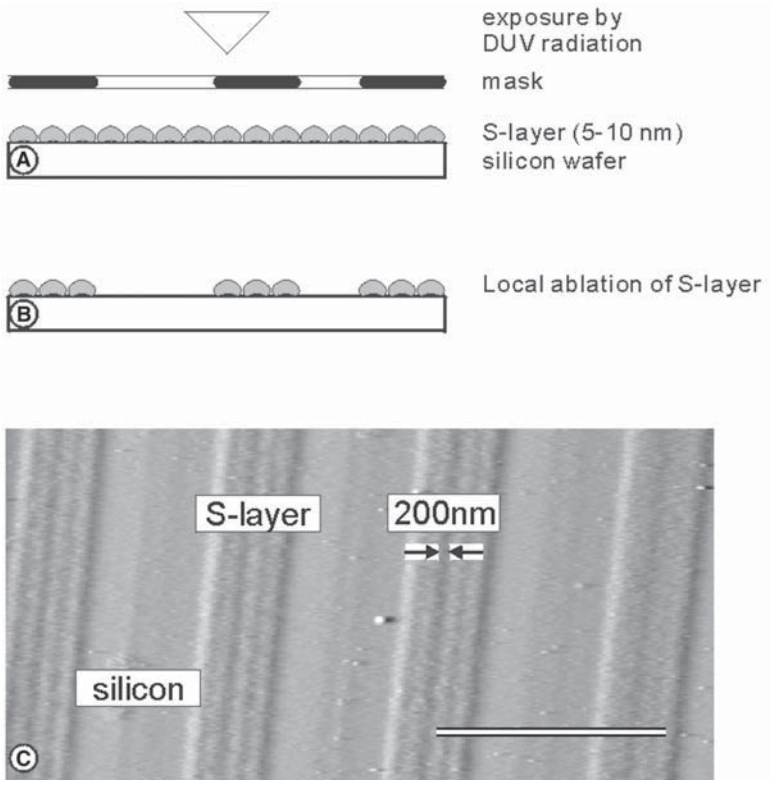

Fig. 5. Schematic drawing of patterning of S-layers by exposure to deep ultraviolet (DUV) radiation. **(A)** A pattern is transferred onto the S-layer by exposure to ArF excimer laser radiation through a microlithographic mask. **(B)** The S-layer is specifically removed from the silicon surface in the exposed areas. **(C)** A scanning force microscopic image of a patterned S-layer on a silicon wafer is shown. Bar = 3 µm. (Modified after **ref. *5*** with permission from the publisher; © 1999, Wiley-VCH.)

metallization prior to subsequent reactive ion etching. Since S-layers are only 5 to 10 nm thick, and thus much smaller than conventional resists (500–1000 nm mean thickness), proximity effects are strongly reduced, yielding a considerable improvement in edge resolution. For the development of bioanalytical sensors, patterned S-layers may also be used as electrode structures for binding biologically active molecules at specified target areas.

3.3.2. Soft Lithography Patterning

A well-known soft lithography technique, micromolding in capillaries (MIMIC) ***(19,20)***, can be used for patterning and self-assembly of 2D S-layer protein arrays on silicon supports. For mold formation, 6-µm-high mesa-struc-

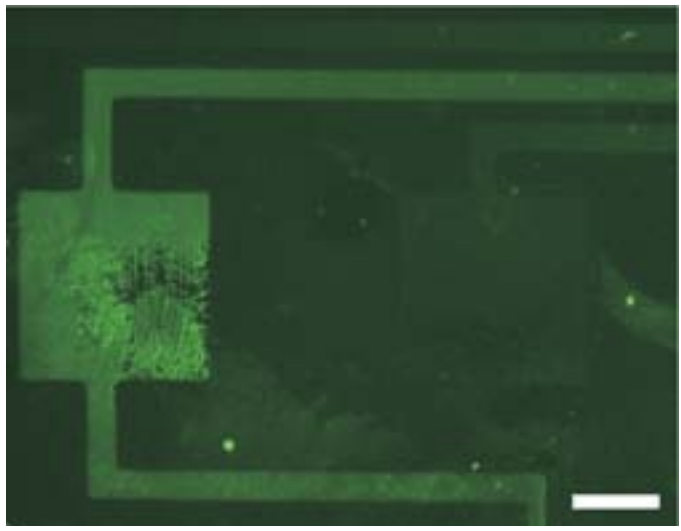

Fig. 6. Fluorescence image of FITC-labeled S-layer protein SbpA patterned at a plasma-treated native silicon oxide support using a PDMS mold. Bar = 50 µm.

ture mold masters were fabricated in photoresist on 4-in. silicon wafers using photolithography. PDMS was used to generate the molds from the masters ***(21,22)***. Ten parts of PDMS and one part of elastomer were mixed and degassed in an exsiccator. The PDMS solution was put on the master, which was placed in a Petri dish, and again the solution was degassed until no bubbles were observed. The PDMS mold was baked at 50°C for at least 4 h and subsequently removed from the master and cut to a proper size. Microchannels were formed when the recessed grooves in the PDMS mold were brought into conformal contact with the planar support, typically a native oxide–terminated silicon wafer.

The microchannels were subsequently filled from one end with protein solution (0.1 mg/mL of SbpA in buffer C) by capillary action. The silicon supports (solvent cleaned) were O_2 plasma treated before application of the mold in order to increase the wettability of the surface and to improve channel filling (*see* **Note 7**). After self-assembly and crystallization of the S-layer protein (30 min to 24 h), the PDMS mold was removed under Milli-Q water, leaving the patterned S-layer arrays on the support. The patterning was detected either by AFM (*see* **Subheading 3.2.**) or by epifluorescence microscopy.

For microscopic detection of fluorescence, the protein structures were labeled with FITC (*see* **Note 8**). The solid-supported S-layer patterns were incubated with the FITC suspension (1 mg of FITC in 100 µL of DMSO, diluted with 2 mL of buffer D) for 1 h at room temperature in the dark. After labeling,

the samples were washed with buffer D and, finally, the patterning was investigated by epifluorescence microscopy (**Fig. 6**).

The MIMIC technique can be utilized for lateral patterning of simple and moderately complex crystalline S-layer arrays ranging in critical dimension from submicrons to hundreds of microns. Furthermore, the native chemical functionality of the S-layer protein is completely retained, as demonstrated by attachment of human IgG antibody and subsequent binding of anti–human IgG antigen on the patterned S-layer substrates ***(23)***. This versatile MIMIC patterning technique can also be combined with immobilization techniques (*see* **Subheading 3.4.**), such as for controlled binding of nanoparticles with well-defined locations and orientations.

3.4. Formation of Nanoparticle Arrays

3.4.1. Preparation of Supports

To obtain comparable surface properties with those of silicon wafers, standard formvar- and carbon-coated electron microscope grids were coated with a 1- to 10-nm-thick layer of SiO_2 by evaporation and subsequent O_2 plasma treatment as described before (*see* **Subheading 3.2.**).

3.4.2. S-Layer Recrystallization

A solution of SbpA of *B. sphaericus* CCM 2177 (0.1 mg of SbpA/mL of buffer C) was used to fill glass wells. Subsequently, the SiO_2-coated grids were placed horizontally at the liquid-air interface and removed after 4 h. In most cases, there was not only a crystalline SbpA layer on the grid but also adsorbed self-assembly products. The S-layer protein-coated grids were washed and stored in Milli-Q water at 4°C.

3.4.3. Nanoparticles

Citrate-stabilized gold nanoparticles with a mean diameter of 5 nm were negatively charged. The amino-modified, positively charged CdSe nanoparticles were prepared according to the literature ***(24,25)*** (*see* **Note 9**). For noncovalent, electrostatic binding of nanoparticles to S-layer lattices, SbpA-coated grids (with or without attached S-layer self-assembly products; *see* **Note 4**) were incubated in the nanoparticle solution for 1 h at room temperature and washed with Milli-Q water.

3.4.4. Transmission Electron Microscopy

Transmission electron microscopy (TEM) analysis was performed on negatively stained but most frequently on untreated preparations. The structural (lattice constants, symmetries) and chemical diversity (surface-active functional groups) of S-layer proteins allows the formation of nanocrystal

superlattices with a spatially controlled packing. Owing to electrostatic interactions, anionic citrate-stabilized gold nanoparticles (5 nm in diameter) formed a superlattice at those sites where the inner face of the S-layer lattice was exposed. By contrast, cationic semiconductor nanoparticles (such as amino functionalized CdSe particles) formed arrays on the outer face of the solid-supported S-layer lattices ***(26)***.

3.5. S-Layer-Supported Lipid Membranes

3.5.1. Formation of Painted Lipid Membranes

Lipid membranes (**Fig. 7A**) were made from a 1% (w/w) solution of DPhyPC in *n*-decane ***(27,28)***. The stock solution was stored at –20°C. The orifice was prepainted with DPhyPC dissolved in chloroform (10 mg/mL) and dried with nitrogen for at least 20 min. Subsequently, the compartments were filled with the electrolyte (12 mL each). The *cis* cell was grounded, and the *trans* cell was connected by another Ag/AgCl electrode to the patch-clamp amplifier. A drop of lipid mixture was put on the Teflon brush and stroked up the orifice. Membrane formation should be seen immediately (*see* **Note 10**). Thinning of the membranes was followed by measuring the capacitance of the lipid membrane. After a constant capacitance was reached (takes approx 20–40 min), experiments to study the intrinsic parameters of the lipid membrane were performed.

3.5.2. Formation of Folded Lipid Membranes

DPhyPC was dissolved in *n*-hexane/ethanol (9:1). The stock solution was stored at –20°C at a concentration of 5 mg of lipid/mL. At least 30 min before the formation of the membrane, the aperture was preconditioned with a small drop of hexadecane/pentane (1:10) (**Fig. 7B**). Both compartments were filled to just below the aperture with electrolyte ***(29)***. A volume of 2 µL of the lipid stock solution was spread on the aqueous surface of each compartment, and the solvent was allowed to evaporate for at least 20 min. Raising the level of the electrolyte within the compartments to above the aperture by means of the syringes led to formation of a lipid membrane, which was checked by measuring its conductance and capacitance (*see* **Note 11**).

The current response from given voltage functions was measured to provide the capacitance and conductance of the lipid membranes ***(30,31)***. A triangular voltage function (+40 to –40 mV, 20 ms) may be used to determine the capacitance of the lipid membrane. The specific capacitance is about 0.4 to 0.5 and 0.6 to 0.8 µF/cm^2 for the painted and folded membranes, respectively ***(9,11,32,33)*** (*see* **Note 12**). Membrane conductance is usually $<10^{-8}$ S/cm^2. The settings of the two built-in Bessel filters of the amplifier for the current monitor signal were 10 and 1.5 kHz, respectively. All experiments should be performed at room temperature (*see* **Note 13**). After each experiment, the Teflon aperture

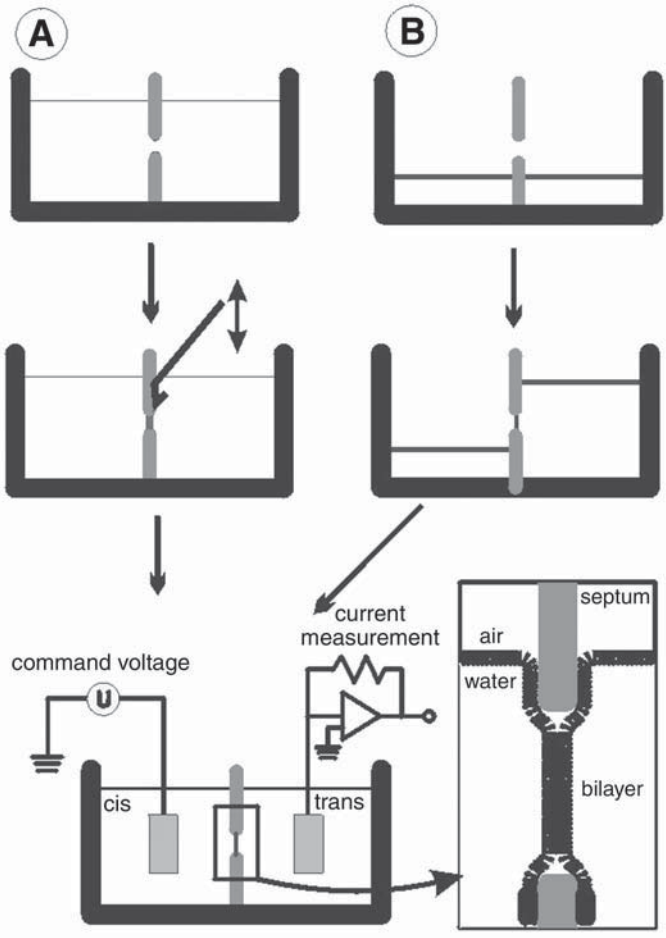

Fig. 7. Schematic illustration of formation of **(A)** painted and **(B)** folded lipid membrane. On the lower left is an illustration of the setup (not drawn to scale), and the inset shows a drawing of the bilayer lipid membrane.

was cleaned extensively with chloroform, methanol, and ethanol and finally rinsed with Milli-Q water.

3.5.3. Recrystallization of S-Layer Proteins SbpA and SbsB

After forming the painted or folded lipid membrane, the S-layer solution was carefully injected into the *trans* compartment to a final protein concentration of 0.1 mg/mL. The same volume of buffer was added to the *cis* compartment. According to our experience, the recrystallization process of S-layer subunits on lipid membranes was generally completed within 3 h ***(34)***. If the

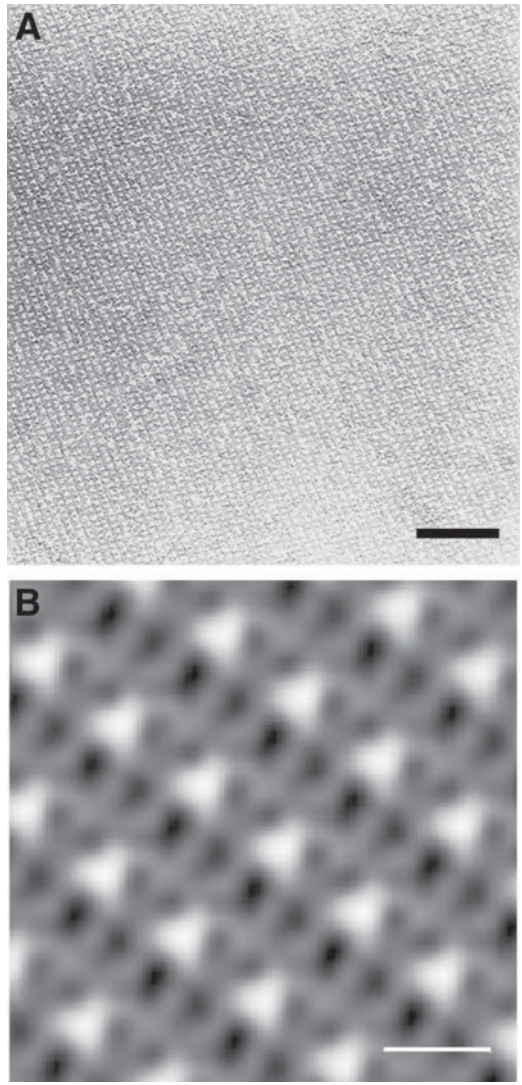

Fig. 8. **(A)** Electron micrograph of negatively stained preparation of S-layer protein SbsB isolated from *G. stearothermophilus* PV72 recrystallized on a monolayer made of DPhPC/hexadecylamine (molar ratio of 10:4). Bar = 100 nm. **(B)** Computer image reconstitution of transmission electron microscopic images of oblique S-layer lattice of SbsB. Bar = 10 nm. (Reprinted from **ref. *35*** with permission; © 2002, Elsevier Science.)

lipid membrane should be supported by the S-layer protein SbpA from *B. sphaericus* CCM 2177, 10 m*M* $CaCl_2$ has to be added to the electrolyte to make recrystallization possible. On the other hand, no $CaCl_2$ is needed for the recrystallization of the S-layer SbsB protein of *G. stearothermophilus* PV72 (**Fig. 8**). The closely attached S-layer lattice did not affect the specific capacitance, whereas the resistance of the membranes increased slightly ***(32,35–38)***. Recrystallization of the S-layer protein can be investigated by TEM (*see* **Subheading 2.4.3.**) on deposited negatively stained preparations or by AFM investigations (*see* **Subheading 2.2.4.**) of the lipid-coated polymer septum.

The advantages of S-layer-supported lipid membranes are the enhanced long-term stability ***(37,38)***; the stability against voltage ramps even up to 500 mV and more ***(39)***; the increased bending stiffness ***(40)***; and, hence, the higher robustness against hydrostatic pressure gradients ***(34,35)***. Thus, it might be possible to distinguish at mechanosensitive ion channels ***(41–43)***, reconstituted in S-layer-supported lipid membranes, between the curvature-induced mechanical activation and the flow-induced activation ***(35)***. In addition, the tightly attached S-layer lattice allows complete reconstitution of membrane-active peptides ***(37,44)*** but also of complex membrane proteins such as α-hemolysin ***(36,38,39)***.

4. Notes

1. For chlorination, immerse silver wire as anode in a 0.1 *N* HCl solution and pass a current of 10 mA for 5 min through the wire.
2. *B. sphaericus* CCM 2177 tends to make the medium alkaline and, thus, one has to be prepared to add H_2SO_4 early enough to maintain a pH of 7.2.
3. The S-layer-containing solutions should be dialyzed against large volumes, usually 3 L of distilled water, with or without $CaCl_2$ taken at each dialysis step. Be sure to cool the distilled water to 4°C before performing dialysis.
4. Single isolated S-layer subunits from many prokaryotic organisms have shown the ability to assemble into regular lattices identical to those observed on intact cells on removal of the disrupting agents used for their isolation (e.g., on dialysis). The S-layer self-assembly processes lead to the formation of flat sheets, open-ended cylinders, or spheres. Ionic strength, temperature, protein concentration, and polymer associated with S-layers can determine both the rate and extent of assembly (for a review, *see* **refs. *5–8***).
5. Excess water has to be carefully removed before patterning in order to prevent interference fringes caused by the water film.
6. S-layer protein is completely removed by ArF (λ = 193 nm) irradiation at a dose of 100 to 200 mJ/cm^2.
7. Rapid filling of the micron-scale channels may be followed with an optical microscope, and capillaries may be filled even when the solution enters from both ends of the mold.

8. FITC binds to the free amino groups of the S-layer protein.
9. The amino-modified CdSe nanoparticles were prepared by an organometallic synthesis using a mixture of highly boiling primary aminoalkanes and trioctylphosphine as the coordinating solvent. The CdSe nanocrystals from about 1 mL of freshly prepared sol were precipitated by adding a small amount of methanol. After removal of the supernatant, the particles were transferred in 5 mL of aqueous solution of 20 m*M* *N*,*N*-dimethyl-mercaptoethylammonium chloride and 1 m*M* 2-(butylamino)-ethanthiol in the case of an additional functionalization with a secondary amine. Five minutes of ultrasonic treatment led to an optically clear solution.
10. Push the Teflon brush very tightly against the septum when the lipid is stroked up the orifice. If the membrane ruptures, try it again with the Teflon brush without dropping new lipid on it.
11. If no membrane formation can be achieved, remove the lipid of the air-water interface using a suction pump, and try it again with a smaller amount of lipid. In addition, be very careful that all solutions and the electrolytes are free of any dust or other contaminants.
12. The dielectric constant for lipid membranes is taken as $\varepsilon = 2.1$, corresponding to the average dielectric constant of a long-chain hydrocarbon.
13. If the humidity is too high or the weather is sultry, membrane formation is very rare and the membranes are usually not very stable.

Acknowledgments

This work was supported by the Ludwig Boltzmann Society; by grants from the Austrian Science Foundation (projects P-14419-MOB and P-16295-B07); and by the Volkswagen Foundation, Germany (project I/77 710).

References

1 Sleytr, U. B., Messner, P., Pum, P., and Sára, M. (eds.) (1996) *Crystalline Bacterial Cell Surface Proteins*, Academic, Austin, TX.
2. Sleytr, U. B. (1978) Regular arrays of macromolecules on bacterial cell walls: structure, chemistry, assembly and function. *Int. Rev. Cytol.* **53,** 1–64.
3 Pum, D., Sára, M., and Sleytr, U. B. (1989) Structure, surface charge, and self-assembly of the S-layer lattice from *Bacillus coagulans* E38-66. *J. Bacteriol*. **171,** 5296–5303.
4. Sára, M., Pum, D., and Sleytr, U. B. (1992) Permeability and charge-dependent adsorption of the S-layer lattice from *Bacillus coagulans* E38-66. *J. Bacteriol.* **174,** 3487–3493.
5 Sleytr, U. B., Messner, P., Pum, D., and Sára, M. (1999) Crystalline bacterial cell surface layers (S layers): from supramolecular cell structure to biomimetics and nanotechnology. *Angew. Chem. Int. Ed.* **38,** 1034–1054.
6. Sleytr, U. B., Sára, M., and Pum, D. (2000) Crystalline bacterial cell surface layers (S-layers): a versatile self-assembly system, in *Supramolecular Polymerization* (Ciferri, A., ed.), Marcel Dekker, New York, pp. 177–213.

7. Sleytr, U. B., Sára, M., Pum, D., and Schuster, B. (2001) Molecular nanotechnology and nanobiotechnology with two-dimensional protein crystals (S-layers), in *Nano-Surface Chemistry* (Rosoff, M., ed.), Marcel Dekker, New York, pp. 333–389.
8. Sleytr, U. B., Sára, M., Pum, D., Schuster, B., Messner, P., and Schäffer, C. (2003) Self assembly protein systems: microbial S-layers, in *Biopolymers*, vol. 7 (Steinbüchel, A. and Fahnestock, S., eds.), Wiley-VCH, Weinheim, Germany, pp. 285–338.
9. Hanke, W. and Schlue, W. R. (1993) Planar lipid bilayers: methods and applications, in *Biological Techniques Series* (Sattelle, D. B., ed.), Academic, London, UK, pp. 24–43.
10. Alvarez, O. (1986) How to set up a bilayer system, in *Ion Channel Reconstitution* (Miller, C., ed.), Plenum, New York, pp. 115–130.
11 Benz, R., Fröhlich, O., Läuger, P., and Montal, M. (1975) Electrical capacity of black lipid films and of lipid bilayers made from monolayers. *Biochim. Biophys. Acta* **394,** 323–334.
12 Montal, M. (1974) Formation of bimolecular membranes from lipid monolayers. *Methods Enzymol.* B **32,** 545–554.
13. Messner, P., Hollaus, F., and Sleytr, U. B. (1984) Paracrystalline cell wall surface layers of different *Bacillus stearothermophilus* strains. *Int. J. Syst. Bacteriol.* **34,** 202–210.
14 Sleytr, U. B., Sára, M., Küpcü, Z., and Messner, P. (1986) Structural and chemical characterization of S-layers of selected strains of *Bacillus stearothermophilus* and *Desulfotomaculum nigrificans*. *Arch. Microbiol.* **146,** 19–24.
15 Bartelmus, W. and Perschak, F. (1957) Schnellmethode zur Keimzahlbestimmung in der Zuckerindustrie. *Z. Zuckerind.* **7,** 276–281.
16 Pum, D. and Sleytr, U. B. (1995) Anisotropic crystal growth of the S-layer of *Bacillus sphaericus* CCM 2177 at the air/water interface. *Colloids Surf. A* **102,** 99–104.
17 Pum, D., Stangl, G., Sponer, C., Fallmann, W., and Sleytr, U. B. (1997) Deep ultraviolet patterning of monolayers of crystalline S-layer protein on silicon surfaces. *Colloids Surf. B* **8,** 157–162.
18 Pum, D., Stangl, G., Sponer, C., Riedling, K., Hudek, P., Fallmann, W., and Sleytr, U. B. (1997) Patterning of monolayers of crystalline S-layer proteins on a silicon surface by deep ultraviolet radiation. *Microelectron. Eng.* **35,** 297–300.
19 Xia, Y. and Whitesides, G. M. (1998) Soft lithography. *Angew. Chem. Int. Ed.* **37,** 550–575.
20 Michel, B., Bernard, A., Bietsch, A., et al. (2001) Printing meets lithography: soft approaches to high resolution patterning. *IBM J. Res. Dev.* **45,** 697–719.
21. Kumar, A., Biebuyck, H. A., and Whitesides, G. M. (1994) Patterning self-assembled monolayers: applications in materials science. *Langmuir* **10,** 1498–1511.
22. Kim, E., Xia, Y., and Whitesides, G. M. (1995) Making polymeric microstructures: capillary micromolding. *Nature* **376,** 581–584.
23. Györvary, E. S., O'Riordan, A., Quinn, A. J., Redmond, G., Pum, D., and Sleytr, U. B. (2003) Biomimetic nanostructure fabrication: nonlithographic lateral

patterning and self-assembly of functional bacterial S-layers at silicon supports. *Nano Lett.* **3,** 315–319.
24 Talapin, D. V., Rogach, A. L., Kornowski, A., Haase, M., and Weller, H. (2001) Highly luminescent monodisperse CdSe and CdSe/ZnS nanocrystals synthesized in a hexadecylamine-trioctylphosphine oxide-trioctylphospine mixture. *Nano Lett.* **1,** 207–211.
25 Talapin, D. V., Rogach, A. L., Mekis, I., Haubold, S., Kornowski, A., Haase, M., and Weller, H. (2002) Synthesis and surface modification of amino-stabilized CdSe, CdTe and InP nanocrystals. *Colloids Surf. A* **202,** 145–154.
26. Györvary, E., Schroedter, A., Talapin, D. V., Weller, H., Pum, D., and Sleytr, U. B. (2004) Formation of nanoparticle arrays on S-layer protein lattices. *J. Nanosci. Nanotechnol.* **4,** 115–120.
27 Mueller, P., Rudin, D. O., Tein, H. T., and Wescott, W. C. (1962) Reconstitution of cell membrane structure *in vitro* and its transformation into excitable systems. *Nature* **194,** 979–981.
28. Fettiplace, R., Gordon, L. G. M., Hladky, S. B., Requena, J., Zingsheim, H. P., and Haydon, D. A. (1975) Techniques in formation and examination of black lipid bilayer membranes, in *Methods of Membrane Biology*, vol. 4 (Korn, E. D., ed.), Plenum, New York, pp. 1–75.
29 Montal, M. and Mueller, P. (1972) Formation of bimolecular membranes from lipid monolayers and a study of their electrical properties. *Proc. Natl. Acad. Sci. USA* **69,** 3561–3566.
30. Darszon, A. (1983) Strategies in the reassembly of membrane proteins into lipid bilayer systems and their functional assay. *J. Bioenerg. Biomembr.* **15,** 321–334.
31 Schindler, H. (1989) Planar lipid-protein membranes: strategies of formation and of detection dependencies of ion transport functions on membrane conditions. *Methods Enzymol.* **171,** 225–253.
32. Schuster, B. and Sleytr, U. B. (2000) S-layer supported lipid membranes. *Rev. Mol. Biotechnol.* **74,** 233–254.
33 Tien, H. T. and Ottova, A. L. (2001) The lipid bilayer concept and its experimental realization: from soap bubbles, kitchen sink, to bilayer lipid membranes. *J. Membr. Sci.* **189,** 83–117.
34 Schuster, B., Sleytr, U. B., Diederich, A., Bähr, G., and Winterhalter, M. (1999) Probing the stability of S-layer-supported planar lipid membranes. *Eur. Biophys. J.* **28,** 583–590.
35 Schuster, B. and Sleytr, U. B. (2002) The effect of hydrostatic pressure on S-layer supported lipid membranes. *Biochim. Biophys. Acta* **1563,** 29–34.
36 Schuster, B. and Sleytr, U. B. (2002) Single channel recordings of α-hemolysin reconstituted in S-layer-supported lipid bilayers. *Bioelectrochemistry* **55,** 5–7.
37 Schuster, B., Pum, D., and Sleytr, U. B. (1998) Voltage clamp studies on S-layer-supported tetraether lipid membranes. *Biochim. Biophys. Acta* **1369***,* 51–60.
38 Schuster, B., Pum, D., Braha, O., Bayley, H., and Sleytr, U. B. (1998) Self-assembled α-hemolysin pores in an S-layer-supported lipid bilayer. *Biochim. Biophys. Acta* **1370,** 280–288.

39. Schuster, B., Pum, D., Sára, M., Braha, O., Bayley, H., and Sleytr, U. B. (2001) S-layer ultrafiltration membranes: a new support for stabilizing functionalized lipid membranes. *Langmuir* **17,** 400–503.
40 Hirn, R., Schuster, B., Sleytr, U. B., and Bayerl, T. M. (1999) The effect of S-layer protein adsorption and crystallization on the collective motion of a lipid bilayer studied by dynamic light scattering. *Biophys. J.* **77,** 2066–2074.
41 Chang, G., Spencer, R. H., Lee, A. T., Barclay, M. T., and Rees, D. C. (1998) Structure of the MscL homolog from *Mycobacterium tuberculosis*: a gated mechanosensitive ion channel. *Science* **282,** 2220–2226.
42 Jones, S. E., Naik, R. R., and Stone, M. O. (2000) Use of small fluorescent molecules to monitor channel activity. *Biochem. Biophys. Res. Commun.* **279,** 208–212.
43 Booth, I. R. and Louis, P. (1999) Managing hypoosmotic stress: aquaporins and mechanosensitive channels in *Escherichia coli*. *Curr. Opin. Microbiol*. **2,** 166–169.
44. Schuster, B., Weigert, S., Pum, D., Sára, M., and Sleytr, U. B. (2003) New method for generating tetraether lipid membranes on porous supports. *Langmuir* **19,** 2392–2397.
45. Sleytr, U. B., Sára, M., Pum, D., and Schuster, B. (2001) Characterization and use of 2D protein crystals (S-layers). *Prog. Surf. Sci.* **68,** 231–278.